Experimental and Theoretical Analysis of the Alkali Impregnation of Eucalyptus Wood

Maria C. Inalbon,*,† Miguel C. Mussati,‡ and Miguel A. Zanuttini†

ITC, Instituto de Tecnología Celulósica (FIQ-UNL), Sgo. del Estero 2654 (S3000AOJ), and INGAR Instituto de Desarrollo y Diseño (CONICET-UTN), Avellaneda 3657 (S3002GJC), Sante Fe, Argentina

Wood impregnation is crucial in any pulping process. The impregnation of chips of eucalyptus wood by a liquor of constant alkali concentration is here analyzed. A mass balance that considers kinetics of the main reactions and a dynamic diffusion coefficient is applied for the six chemical species analyzed. The diffusion rate is assumed dependent on temperature, alkali concentration, and the advance degree of reactions. The predicted concentration profiles are in acceptable agreement with the experimental results for hidroxyl and sodium ions, as well as for acetyl groups. For each set of impregnation conditions and chip thickness, characteristic impregnation times or impregnation levels can be predicted by the model.

1. Introduction

In the Kraft process or any other alkaline industrial pulping process, wood chips are cooked with alkaline liquor in order to defibrate the material and obtain the pulp. Chips must be properly impregnated with the chemical reagents prior to the cooking, generally in a separate stage. The homogeneity of the whole chemical treatment can be strongly affected by the quality of the alkaline impregnation. Indeed, the favorable effect of an adequate impregnation stage on the final pulp properties has been shown by several authors.[1−5]

The alkali wood impregnation implies the penetration of liquids, diffusion of chemical reagents, and also chemical reactions and swelling. For a detailed analysis of the phenomenon, not only the knowledge of involved reactions and diffusion coefficients in wood but also the information of the impregnation pattern is needed.

The reaction of acetyls and acid groups as well as the "peeling" reaction, all of them on the hemicelluloses, are likely to occur. Nevertheless, the deacetylation is the main reaction involved and it is responsible for a considerable amount of alkali consumed.[6] Deacetylation kinetics for eucalyptus wood under conditions close to impregnation operation has been reported by Inalbon et al.[7]

On the other hand, alkali modifies the local ion transport capacity. Through determination of the effective capillary cross-sectional area, Stone[8] has shown that diffusion in a hardwood in transverse direction is strongly modified by alkalinity. This ion diffusion capillarity is significantly increased when pH is increased from 12.0 to 13.0. In a recent work,[9] a wood effective capillary cross-sectional area dependency with alkalinity, temperature, and chemical reaction degree was experimentally determined.

The reactions, together with the capillarity change, lead to a complex pattern of the alkaline impregnation process. An advancing impregnation front separates an intact inner part of the particle from a swollen outer shell.[10] The existence of this advancing front suggests that the process of diffusion with chemical reaction and swelling can be approximately described by a shrinking core model. This concept was adopted for the comprehensive Kraft pulping modeling carried out by Gustafson et al.[11]

The importance of the chip thickness on the uniformity of the obtained pulp in a Kraft pulping process has been shown for many authors.[1,12−14] Therefore, the chip thickness (radial or tangential wood direction) is the critical dimension for the diffusion processes involved in treatment systems.[1,14] For this reason, a one-dimensional balance along the transverse direction of the wood is an approach useful to understand and quantitatively analyze the phenomenon.

In this paper, a mass balance for the main ions involved is considered. The study takes into account the relevant chemical reactions involved and the temporal changes of the wood properties at each position of the chip due to the alkali action. Profiles of sodium and hydroxide ions, and acetyl groups concentration are compared to experimental results.

2. Experimental Protocol

Green, fresh Eucalytpus grandis wood with an average density of 0.366 g/cm^3 was used. Six-year old logs were supplied by INTA-Concordia, Argentina.

Acid Group Determination. The acid group content was determined by conductometric titration[15] on extractive-free milled wood retained in a 60-mesh sieve. Original and treated wood (45 °C in an alcoholic alkaline solution, pH 12.5) was analyzed as representative of the initial and the total acid group content, respectively. Table 1 shows the original and the increase in acid groups content that alcoholic alkaline treatment produced which correspond to the un-ionized in the original wood.

Experimental Impregnation Profiles. The impregnation profile was obtained using wood blocks of 3.5 cm side. In a closed reactor, those blocks were steamed and then sunk in the

Table 1. Content of Ionized Acid Group and Un-ionized Acid Group (Ester, Lactone, and Acid Forms) in the Original Wood (meq/kg)[a]

ionized acid groups	un-ionized acid groups	acetyl groups	un-ionized acids/ acetyls ratio
82.5	198.1	907	0.21

[a] The original content of acetyl group (meq/kg) and the ratio between alkali reactive acid group and acetyl content is indicated; 907 meq acetyl /kg = 3.9% acetyl on wood.

* To whom correspondence should be addressed. E-mail: cinalbon@fiq.unl.edu.ar. Tel./Fax: +54-342-4520019.

† ITC, Instituto de Tecnología Celulósica.

‡ INGAR Instituto de Desarrollo y Diseño.

10.1021/ie801685a CCC: $40.75
Published on Web 04/08/2009

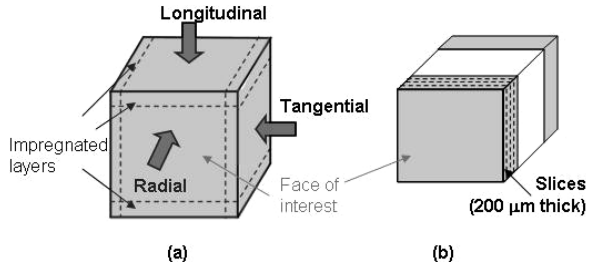

Figure 1. Scheme of the wood block: (a) alkali impregnated, (b) prepared for radial slicing.

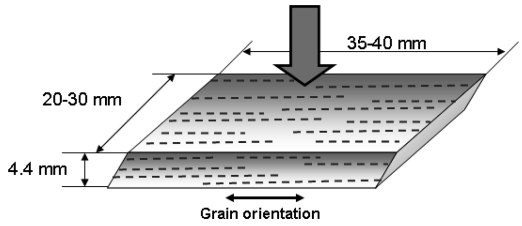

Figure 2. Scheme of the direction of impregnation analyzed.

impregnation liquor; immediately after that, the pressure of the system was increased to 0.6 MPa. Blocks were kept under pressure and agitation. Once the treatment time was reached, the pressure was relieved; the blocks were taken off the reactor, and immediately immersed into liquid nitrogen. Then, they were stored in a freezer at −10 °C. The procedure is described in greater detail elsewhere.[16]

The frozen blocks were sliced with a carpentry saw to remove the layers of impregnated wood, with the exception of the faces of interest (radial faces) (Figure 1a). Those faces were then cut into 200 μm-thick serial slices (Figure 1b). For the analysis of slices, a procedure previously used to study poplar impregnation was followed.[10]

Slices were weighed, and their alkali content was determined by quantitative neutralization of 20 mL of water containing the slice. In the liquid volume resulting from neutralization, sodium concentration was determined by atomic absorption spectroscopy (SM 3500-Na) and acetate concentration by gas chromatography (packed column: 10% Carbowax in chromosorb, column temperature = 90 °C). The content of sodium and acetate in the slice was calculated from these concentrations. The acetyl group content was determined on air-dried slices using a modification of the method proposed by Solar et al.[17] The acetyl content of original wood is shown in Table 1.

3. Model Description

The isothermal and unidirectional alkali impregnation through the thickness of the chip (Figure 2) for constant alkali concentration in the impregnation liquor is here analyzed.

The species considered are sodium ion, hydroxyl ion, and acetate ion, all of them in the liquid medium, as well as acetyl group and acid group which are fixed in the wood. Sodium is considered the only positive ion present.

Industrial impregnation is normally performed after chip steaming. A proper steaming preheats the wood and displaces the air from the interior cavities. Wood heats up rapidly and the vapor generated inside the material favors significantly the displacement of air.[18]

In a previous work,[19] it was shown that the steaming stage followed by a pressurized impregnation leads to a liquid saturation of the wood. This liquid content can be ascribed to steam condensation in voids during steaming as well as to the liquor penetration.

Assuming liquid saturation of wood, the alkali impregnation through the chip thickness here analyzed can be considered as a reacting nonconvective diffusion process. Furthermore, under this assumption, the solid material can be considered as a pseudohomogeneous solid with local uniform properties, which are a combination of both the solid and liquid properties. The derived model is able to straightforward incorporate other chemical species present in the Kraft pulping in order to obtain a more rigorous process representation.

Reactions and Kinetic Expression. The kinetic expression of eucalyptus wood deacetylation has been previously determined[7] for a temperature range between 20 and 90 °C, and an alkali concentration range between 0.01 and 0.1 N NaOH. The expression considers the effect of the ionic strength through sodium concentration.

$$R = R_{\text{acetyls}} = k(c_{\text{acetyls}})^n(c_{\text{OH}})^m(c_{\text{Na}})^p \tag{1}$$

where R_i is the chemical consumption or generation rate of ion i (mol/(L·min)), k is the specific reaction rate constant, c_i is the concentration of ion i (mol/L), and n, m, and p are reaction orders.

To our knowledge, there is no information about the hydrolysis rate of esters and lactones of the acid groups. The neutralization is very fast; however, the presence of alkali is required to produce the reaction. All together, these acid group reactions represent one-fifth of the deacetylation (Table 1). Then, the rate of the acid group reactions is here considered to be coupled to the deacetylation rate.

$$R_{\text{IAG}} = -R_{\text{AG}} = \frac{\text{initial acid group}}{\text{initial acetyl group}} R_{\text{acetyls}} \tag{2}$$

where IAG is the ionized acid group, AG is the un-ionized acid group and acetyls is the acetyl groups. The mobility and the alkaline degradation of the hemicelluloses are neglected.

Diffusion Coefficients. Effective ion diffusion coefficients in transverse direction of wood is expressed as a product of the ion diffusion coefficient in a liquid medium and the wood effective capillary cross sectional area (ECCSA) in this direction.

$$D_i = D_{i(\text{in solution})}\text{ECCSA} \tag{3}$$

where D_i is the effective diffusion coefficient of ion i in wood (cm^2/min), $D_{i(\text{in solution})}$ is the diffusion coefficient of ion i in solution (cm^2/min).

Considering the ion mobility (λ^0_i) the diffusion coefficient in a liquid medium is expressed by the Nernst−Einstein equation as

$$D_{i(\text{in solution})} = \frac{RT\lambda_i^0}{\lfloor z_i \rfloor F^2} \tag{4}$$

where R is the universal gas constant (8.3143 J/mol·K), T is the temperature, F is the Faraday constant (96487 J/mol.V), and z_i is the ion valence.

To establish λ^0_i temperature dependences, experimental data from literature[20] were adjusted to linear relations. Fitting (not shown here) was remarkably good for the three ions considered ($R^2 > 0.99$).

The ECCSA in the transverse wood direction is dependent on the alkali concentration, temperature, and reaction degree, which may vary with time. On the basis of the analogy between

capillarity and electrical conductivities of wood, the ECCSA of the eucalyptus wood here under study has been determined using a novel method.[9] It involves the determination of the ratio between the electrical conductivity through the solution saturated wood slices and the conductivity of the solution. This method allows the determination of the wood ECCSA and its change in time, while the wood undergoes the alkali action. It was shown that capillarity depends mainly on the acetyl content and temperature, and it can be modeled by the following expression:[16]

$$\mathrm{ECCSA} = a + b(c_{\mathrm{acetyls}}) - c(c_{\mathrm{acetyls}})^3 - d(c_{\mathrm{acetyls}})T + e(c_{\mathrm{acetyls}})^2T + fT \quad (5)$$

where a, b, c, d, e, and f are empirical coefficients.

Model Derivation. The mass conservation equation is

$$\frac{\partial c_i}{\partial t} + \nabla N_i = R_i \quad (6)$$

where t is the time (min), N_i is the molar net flux of ion i (mol·cm/(L·min))

$$N_i = -\frac{D_i}{RT}c_i\nabla\mu_i + c_i v \quad (7)$$

where μ_i is the electrochemical potential of ion i (J/mol) and v is the solution velocity (cm/min). Solution does not move, thus $v = 0$.

The potential gradient is[21]

$$\nabla\mu_i = RT\nabla \ln c_i + z_iF\nabla\phi + RT\nabla(\ln \gamma_i) \quad (8)$$

where ϕ is the electric potential (volt) and γ_i is the chemical activity coefficient.

For ideal solution, the molar flux is

$$N_i = -D_i\nabla c_i - \frac{z_iFD_ic_i}{RT}\nabla\phi \quad (9)$$

In this expression (eq 9), the first term of the right-hand side represents the diffusion flux, which is the result of the concentration gradient. The second one represents the migrational flux, which is induced by the potential gradient; this term is the result of the difference on the diffusion coefficients of the ions, which tends to produce a charge distribution.

The condition of zero electric current (i) is considered in order to determine the electric potential gradient.

$$i = F\sum z_iN_i = 0 \quad (10)$$

Replacing eq 9 in eq 10 results in

$$\frac{\partial\phi}{\partial x} = \left(\frac{RT}{F}\right)\frac{-\sum_i z_iD_i\frac{\partial c_i}{\partial x}}{\sum_i z_i^2D_ic_i} \quad (11)$$

Then, the mass balance becomes as follows:

$$\frac{\partial c_i}{\partial t} = \frac{\partial D_i}{\partial x}\frac{\partial c_i}{\partial x} + D_i\frac{\partial^2 c_i}{\partial x^2} + \left(z_iD_i\frac{\partial c_i}{\partial x} + z_ic_i\frac{\partial D_i}{\partial x}\right)\times \left(\frac{-\sum_i z_iD_i\frac{\partial c_i}{\partial x}}{\sum_i z_i^2D_ic_i}\right) + z_iD_ic_i\frac{F}{RT}\frac{\partial}{\partial x}\left(\frac{-\sum_i z_iD_i\frac{\partial c_i}{\partial x}}{\sum_i z_i^2D_ic_i}\right) + R_i \quad (12)$$

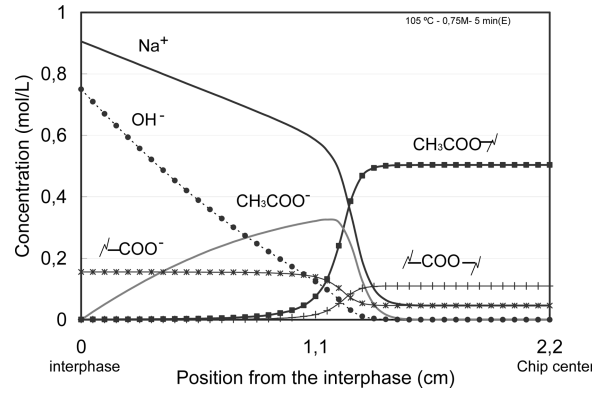

Figure 3. Theoretical concentration profiles obtained for the impregnation of a 4.4 mm thick chip with 0.75 N NaOH at 105 °C for 5 min: (OH) hydroxyl; (Na^+) sodium; (CH_3COO-/) acetyl group; (CH_3COO^-) acetate group; (/-COO^-) ionized acid group; (/-COO-/) acid group esterified or in its acid form.

The following assumptions are considered to set the boundary and initial conditions:

Boundary Conditions. (1) The flux at the chip center is zero. (2) External mass transfer restrictions are neglected at the interphase.

Initial Conditions. (1) The initial concentrations of hydroxyl and acetate ions in the wood are zero. (2) The initial acetyl and acid group content in wood corresponds to an untreated wood content, and the initial sodium content is equal to that hydrolyzed acid group content.

4. Results and Discussion

The resulting equation system was numerically solved using general process modeling system gPROMS, which is a computational environment for modeling, dynamic simulation, and optimization. The concentration profiles of the different chemical species involved were predicted and compared to experimental results.

Figure 3 shows the profiles predicted for an impregnation of a 4.4 mm thick chip with 0.75 N NaOH at 105 °C during 5 min. The figure shows the concentration of the different ions present in a half of the chip (2.2 mm). The figure indicates that profiles of acetyl, ionic acid group, and non-ionic acid group are rather steep. This, in terms of the shrinking core model, is an indication that the reactive processes are faster than the alkali diffusion process.

Sodium concentration is always higher than hydroxyl concentration because the former must be equivalent to the sum of the concentrations of the negative ions: hydroxyl, acetate, and ionic acid groups.

Since the hydroxyl ion diffuses from the interphase to the chip center and is chemically consumed, its concentration profile shows a gradual reduction from the external level to a null concentration in the impregnation front. Acetate ion diffuses forward but mainly backward to the interphase.

Figure 4 shows experimental and simulated sodium, acetyl, and hydroxyl concentrations at different distances from the interphase. It can be observed that the model predictions are satisfactory. A transition zone ranging from 0.55 to 0.95 mm can be defined in this case. These limits are indicated in the figure by dashed vertical lines. In the inner zone, there is no presence of alkali and the acetyl content takes the level of the untreated wood 0.5 N, which corresponds to a 3.9% on oven dry wood. Behind the transition zone, there is no presence of acetyl groups. The transition zone can be considered as a moving

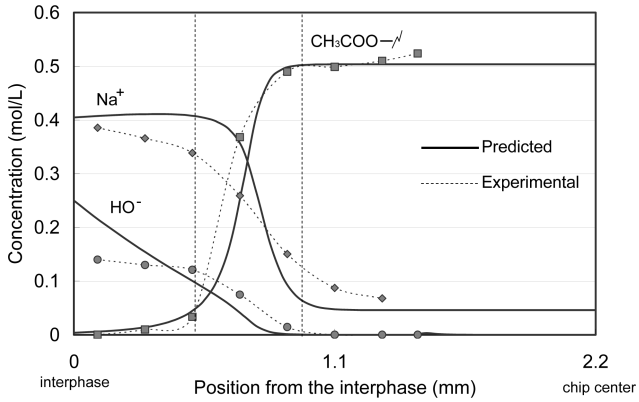

Figure 4. Experimental values of sodium, acetyl, and hydroxyl concentrations and the predicted profiles for a impregnation with 0.25 N NaOH, at 105 °C during 5 min.

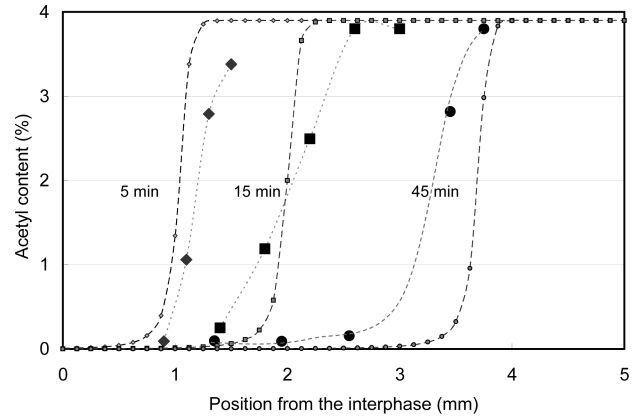

Figure 5. Experimental and predicted acetyl concentration profiles for an impregnation with 0.5 N NaOH, at 110 °C for 5, 15, and 45 min.

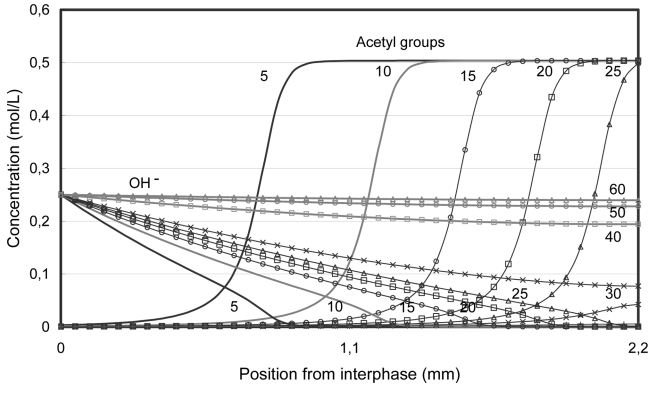

Figure 6. Evolution of the hydroxyl and acetyls group concentration in a 4.4 mm thick chip when impregnating with 0.25 N NaOH at 110 °C. Times are indicated in min.

impregnation front, whose position at different times allows determining the pace of impregnation.

Figure 5 shows the experimental and predicted acetyl concentration profile for a 10 mm thick chip, impregnated with NaOH 0.5 N at 110 °C for 5, 15, and 45 min. The acetyl content looks like a sigmoid-shaped profile moving toward the chip center. The model predictions are acceptable when compared to experimental measurements.

Figure 6 shows the predicted temporal evolution from 5 to 60 min for hydroxyl and acetyl group concentration along the thickness of a 4.4 mm thick chip impregnated with 0.25 N NaOH at 110 °C. Again, the acetyl content looks like a sigmoid-shaped profile moving toward the chip center.

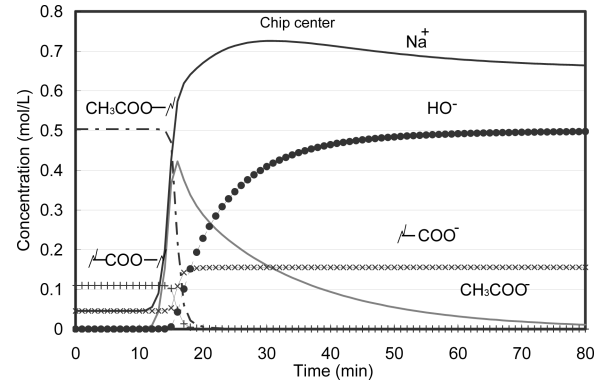

Figure 7. Concentration of different ions in the center of a 4.4 mm thick chip when impregnating with 0.5 N NaOH at 110 °C.

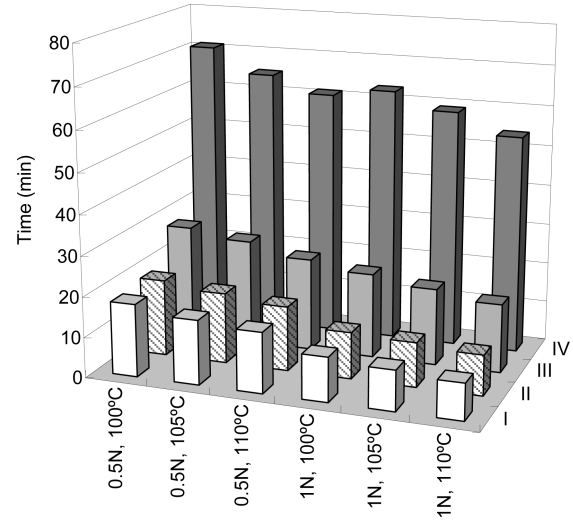

Figure 8. Characteristic impregnation times for a 4.4 mm thick chip: (I) alkali arrival; (II) 50% deacetylation; (III) 100% deacetylation; (IV) achievement of the external alkali concentration.

For a given chip thickness, the model is able to predict the level of impregnation attained and, thus, it is a useful tool for analyzing the wide thickness distribution of the industrial chips.

Depending on the treatment conditions, characteristic impregnation times can be defined. For instance, for the case analyzed in Figure 6, a zero hydroxyl concentration is computed at the chip center until 25 min. After that, the hydroxyl concentration rapidly rises at that position because the chemical reactions have almost finished and the hydroxyl diffuses from both faces of the chip. Figure 7 shows the evolution of concentration of different ions at the center of a 4.4 mm thick chip impregnated with 0.5 N NaOH at 110 °C.

Four characteristic times can be defined that correspond to the following situations taking place at the middle plane of the chip: (I) alkali arrival; (II) 50% deacetylation; (III) 100% deacetylation; (IV) achievement of the external alkali concentration. The characteristic times corresponding to different external alkali concentrations and temperatures are listed in Figure 8.

Finally, Figure 9 shows the position of the impregnation front (acetyl concentration reduction to 50% of the original level) as a function of time for different treatment conditions. Figure 9 is valid to a chip with a half-thickness of 2.2 mm or lower.

Figure 9 clearly shows that, for the variable ranges investigated, the favorable effect of increasing the concentration is larger than the effect of increasing the temperature.

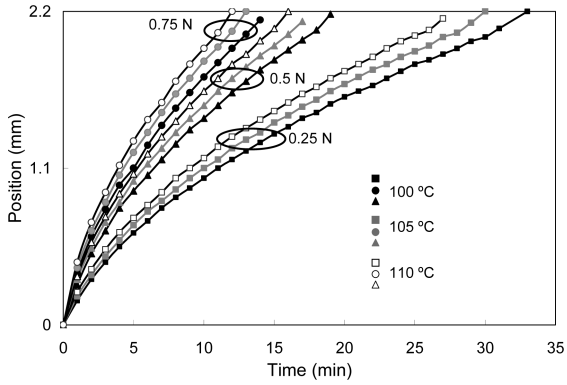

Figure 9. Position of the impregnation front for different treatment conditions as a function of time.

5. Conclusions

The general patterns found for the simulation of the alkali impregnation phenomenon are in acceptably good agreement with experimental results. The derived model is able to incorporate straightforward other chemical species present in the Kraft pulping in order to obtain a more rigorous process representation. The profile of acetyl is always steep, which is an indication that reactive processes are faster than the alkali diffusion process. The profile looks like a sigmoid-shaped profile moving toward the chip center. Alkali concentration is gradually decreasing from the external concentration to the null concentration in the impregnation front. The sodium concentration, which must be equivalent to the sum of the concentrations of the negative ions, is always clearly higher than the hydroxyl concentration.

The effect of the main process variables (external alkali concentration, temperature, time, and chip thickness) can be analyzed through the proposed model. Characteristic impregnation times can be determined for each set of operation conditions. The level of impregnation can be predicted for different thicknesses of an industrial chips stock.

In the range of process variables here investigated, an increase in the concentration speeds up the impregnation process more than an increase in temperature.

Acknowledgment

The authors wish to thank UNL (PI 004-18 2005 Program), ANPCyT (PICTO 14-13231), and Consejo Nacional de Investigaciones Científicas y Técnicas (CONICET) for their financial support.

Literature Cited

(1) Gullichsen, J.; Hyvärinen, R.; Sundquist, H. On the nonuniformity of the Kraft cook Part 2. *Pap. Puu* **1995**, *77* (5), 331.

(2) Höglund, O.; Pehu-Lehtonen, K.; Hjort, A. Kraft pulping with black liquor pretreatment. *TAPPI Proc., Pulp. Conf.* **1994**, 1225–1236.

(3) Malkov, S.; Tikka, P.; Gullichsen, J. Towards complete impregnation of wood chips with aqueous solutions. Part 3: Black liquor penetration into pine chips. *Pap. Puu* **2001**, *83* (8), 605–609.

(4) Svedman, M.; Tikka, P. The use of green liquor and its derivatives in improving Kraft pulping. *Tappi J.* **1998**, *81* (10), 151–158.

(5) Ban, W.; Lucia, L. Enhancing Kraft pulping through unconventional, higher sulfide-containing pretreatment liquors- A review. *Tappi J*. **2003**, *2*.

(6) Zanuttini, M.; Marzocchi, V.; Citroni, M.; Mocchiutti, P. Alkali impregnation of hardwoods. Part I. Moderate treatment of poplar wood. *J. Pulp Pap. Sci.* **2003**, *29* (9), 3131–317.

(7) Inalbon, M. C.; Mocchiutti, P.; Zanuttini, M. A. The deacetylation reaction in eucalyptus wood. Kineti and effects on the effective diffusion. *Bioresour. Technol.* **2009**, *100* (7), 2254–2258.

(8) Stone, J. E. The effective capillary cross-sectional area of word as a function of pH. *Tappi* **1957**, *40* (7), 539–543.

(9) Inalbon, M. C.; Zanuttini, M. A. Dynamics of the effective capillary during the alkaline impregnation of eucaliptus wood. *Holzforschung* **2008**, *62* (4), 397–401.

(10) Zanuttini, M.; Citroni, M.; Marzocchi, V. Pattern of alkaline impregnation of poplar wood at moderate conditions. *Holzforschung* **2000**, *54* (6), 631.

(11) Gustafson, R.; Jimenez, G.; McKean, W. The role of penetration and diffusion in nonuniform pulping of softwood chips. *Tappi J.* **1989**, *72*, 163–167.

(12) Borlew, P.; Miller, R. Chip thickness: A critical dimension in Kraft pulping. *Tappi* **1970**, *53* (11), 2107–2111.

(13) Akhataruzzaman, A. F.; Virkola, N. E. Influence of chip dimensions in Kraft pulping. *Pap. Puu* **1979**, *61* (10).

(14) Gullichsen, J.; Kolehmainen, H.; Sundqvist, H. On the nonuniformity of the Kraft cook. *Pap. Puu* **1992**, *74* (6), 486–490.

(15) Katz, S.; Beatson, R. P.; Scallan, A. M. The determination of strong and weak acidic groups in sulfite pulp. *Svensk Papperstidning.* **1984**, *87* (6), 48–53.

(16) Inalbon M. C. Mecanismo y velocidad de impregnación alcalina de maderas. (Mechanism and rate of alkaline impregnation of wood.) Ph.D. Thesis. FIQ: UNL, Argentina (in Spanish), 2008.

(17) Solár, R.; Kacik, F.; Melcer, Y. Simple semi-micromethod for the determination of O-acetyl groups in wood and related materials. *Nord. Pulp Paper Res. J.* **1997**, *2* (4), 139–141.

(18) Malkov, S.; Tikka, P.; Gullichsen, J. Towards complete impregnation of wood chips with aqueous solutions. Part 4. Effects of front-end modifications in displacement batch Kraft pulping. *Pap. Puu* **2002**, *84* (8), 526–530.

(19) Inalbon, M. C.; Zanuttini, M.; Marzocchi, V.; Citroni, M.; Pieck, C. Inpregnação de madeiras de eucalipto e pinho em processos de polpação alcalina, efeitos da pré-vaporização e da impregnação pressurizada. (Impregnation of eucalyptus and pine wood in alkane pulping process. Effects of pre-steaming and pressurized impregnation.) *O Papel* **2005**, 76–82 (in Portuguese).

(20) Robinson, R. A., Stokes, R. H. *Electrolyte Solutions*, 2nd ed. (revised); Butterworths: London, 1959.

(21) Newman, J. *Electrochemical Systems*; Prentice Hall: New York, 1973.

Received for review November 5, 2008
Revised manuscript received February 17, 2009
Accepted March 10, 2009

IE801685A